Atomic Arrangement, Hydrogen Bonding and Structural Com-Plexity of Alunogen, Al2(SO4)3·17H2O, From Kamchatka Geo-Thermal Field

Elena S Zhitova *, Rezeda M Sheveleva, Andrey A Zolotarev, Anton A Nuzhdaev

Posted Date: 10 May 2023

doi: 10.20944/preprints202305.0681.v1

Keywords: alunogen; sulfate; geothermal field; Kamchatka; hydrated; crystal structure; hydrogen bonding; structure complexity; volcano

Article

Atomic Arrangement, Hydrogen Bonding and Structural Complexity of Alunogen, $Al_2(SO_4)_3 \cdot 17H_2O$, from Kamchatka Geothermal Field

Elena S. Zhitova [1,*], Rezeda M. Sheveleva [1,2], Andrey A. Zolotarev [1,3] and Anton A. Nuzhdaev [1]

[1] Institute of Volcanology and Seismology, Far East Branch of Russian Academy of Sciences, Piipa Blvd. 9, 683006 Petropavlovsk-Kamchatsky, Russia
[2] Research part of the Institute of Geosciences, Saint-Petersburg State University, University emb., 7/9, 199034 Saint-Petersburg, Russia
[3] Crystallography department, Saint-Petersburg State University, University emb., 7/9, 199034 Saint-Petersburg, Russia
* Correspondence: zhitova_es@mail.ru

Abstract: Alunogen, $Al_2(SO_4)_3 \cdot 17H_2O$, occurs as an efflorescent in acid mine drainage, low-temperature fumarolic or pseudofumarolic (at coal fires) terrestrial environments. It is considered as one of the main Al-sulfates of Martian soils demanding comprehensive crystal chemical data of natural terrestrial samples. However, structural studies of natural alunogen were carried out in 1970s without localization of H atoms and have not previously been performed for samples from geothermal fields, despite the fact that these environments are considered as proxies of the Martian conditions. The studied alunogen sample comes from Verkhne-Koshelevsky geothermal field (Koshelev volcano, Kamchatka, Russia). Its chemical formula is somewhat dehydrated, $Al_2(SO_4)_3 \times 15.8\ H_2O$. The crystal structure was solved and refined to $R_1 = 0.068$ based on 5112 unique observed reflections with $I > 2\sigma(I)$. Alunogen crystalizes in $P\text{-}1$ space group, a = 7.4194(3), b = 26.9763(9), c = 6.0549(2) Å, α = 90.043(3), β = 97.703(3), γ = 91.673(3) °, V = 1200.41(7) Å^3, Z = 2. The crystal structure consists of isolated SO_4 tetrahedra, $Al(H_2O)_6$ octahedra and H_2O molecules connected by hydrogen bonds. The structure refinement includes Al, S and O positions that are similar to previous structure determinations and thirty-four H positions localized for the natural sample first. The study also shows the absence of isomorphic substitutions in the composition of alunogen despite the iron-enriched environment of mineral crystallization. The variability of the alunogen crystal structure is reflected in the number of "zeolite" H_2O molecules and their splitting. The structure complexity of alunogen and its modifications ranges from 333-346 bits/cell for models with non-localized H atoms to 783-828 bits/cell for models with localized H atoms. The higher values correspond to higher hydration state of alunogen.

Keywords: alunogen; sulfate; geothermal field; Kamchatka; hydrated; crystal structure; hydrogen bonding; structure complexity; volcano

1. Introduction

Alunogen is a hydrated aluminium sulfate with the formula, $Al_2(SO_4)_3 \times 17H_2O$, regarded as grandfathered mineral species because known since 1832 [Beudant, 1832]. Alunogen is rather widely distributed mineral reported as acid mine drainage mineral and low-temperature fumarolic mineral or pseudofumarolic at coal fires [Košek et al., 2018; Bariand et al., 1977; Biagioni et al., 2020; Zhitova et al., 2018; Menchetti, Sabelli, 1974]. The early study of optical properties has shown that they considerably vary depending on H_2O content in the mineral [Larsen, Steiger, 1928]. Rather detailed description of alunogen crystal forms appeared as a result of the Chilian mineralogical expedition of 1938 [Gordon, 1942]. In this study [Gordon, 1942] authors found crystals of alunogen in small cavities

Preprints (www.preprints.org) | NOT PEER-REVIEWED | Posted: 10 May 2023 doi:10.20944/preprints202305.0681.v1

where alums were dissolved and note that the true alunogen is colourless and triclinic which readily dehydrated to white monoclinic mineral designated as meta-alunogen. The first crystal structure refinement of alunogen [Menchetti, Sabelli, 1974] was carried out on crystals from Grotta dell'Allume (or "Alum Cave"), Vulcano Island, Italy (symmetry and unit-cell parameters are given in Table 1) and allowed determination of Al, S and O positions (two Al sites; three S sites and twenty-nine O sites). For clarity we need to note that Grotta dell'Allume locality was representing a tectonic cavity in the volcanic tuff in close proximity to the sea and on the island where the active Vulcano volcano (Italy) is located [Forti et al., 1994]. The conditions of the mineral formation there are more exotic than usually and include a reaction of volcanic fluid with volcanic tuff in the contact with sea water [Forti et al., 1994]. The first structural study of alunogen [Menchetti, Sabelli, 1974] confirmed variation of the H_2O content and converged to the structural formula, $Al_2(SO_4)_3 \times 16.4H_2O$. The symmetry of the mineral (Table 1) and the position of the main atomic sites (for Al, S and O atoms) were confirmed in the result of subsequent structural refinement, performed a couple of years later [Fang, Robinson, 1976]. The refinement converged to the formula, $Al_2(SO_4)_3 \times 17H_2O$ [Fang, Robinson, 1976]. The crystal structure of alunogen consists of isolated SO_4 tetrahedra and isolated $Al(H_2O)_6$ polyhedra interconnected by hydrogen bonding. The H_2O molecules can be separated to two types: (i) those occurring in cavities and being of "zeolitic" nature (5 per formula unit) and (ii) those coordinating Al octahedra (12 per formula unit: 6 for each of two Al sites). In both studies, only oxygen atoms are localized for H_2O molecules. The crystal structure of alunogen is described [Fang, Robinson, 1976] as consisting of pseudo-double sheets parallel to (010) alternating with tetrahedra-water sheet composed of one SO_4 tetrahedra surrounded by H_2O molecules. This leads to perfect cleavage in sheet stacking direction and formation of tabular crystals.

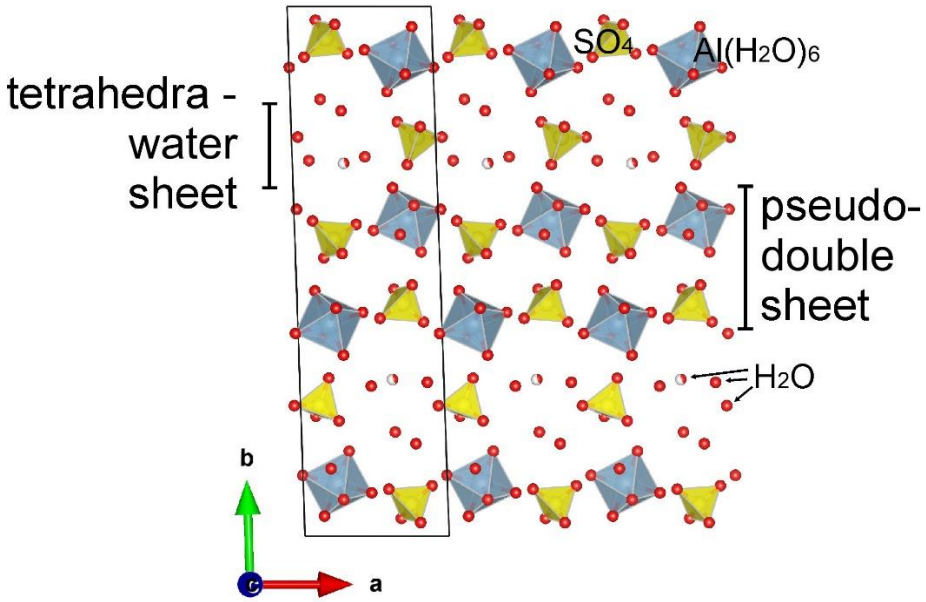

Figure 1. The crustal structure of alunogen obtained by [Menchetti, Sabelli, 1974].

Fang and Robinson [Fang, Robinson, 1976] noted that O sites of H_2O molecules are restricted to 5 leading to 17 H_2O molecules (12 H_2O molecules coordinating Al and other 5 H_2O "zeolite" molecules occurring in sulfate-water sheet) per formula unit. Then the crystal structure of alunogen was obtained on synthetic material [Sun et al., 2015] and topologically agreed with previous observation although the unit-cell setting was different leading to the difference in the unit-cell parameters (Table 1). The crystal structure of synthetic material was supplemented by localization of H atoms [Sun et al., 2015] but according to our analysis geometries of some H_2O molecules do not seem crystal chemically reasonable. Assumptions that Al sulfates are one of the main minerals of Martian Al-bearing soils [Bibring et al. 2006; Swayze et al. 2008; Kounaves et al. 2010; Bish et al. 2013] triggered structure research of alunogen under low- and high-temperature conditions and different

Preprints (www.preprints.org) | NOT PEER-REVIEWED | Posted: 10 May 2023 doi:10.20944/preprints202305.0681.v1

moistures [Kahlenberg et al., 2015, 2017] carried out on synthetic samples. This research has shown that under Mars relevant conditions (low temperature) alunogen undergoes a phase transition to low-temperature monoclinic modification (Table 1), while at slightly elevated temperature of ~ 90 °C partly dehydrated triclinic alunogen-like (or meta-alunogen) material with the formula, $Al_2(SO_4)_3(H_2O)_{12}\cdot 1.8H_2O$, occurred (Table 1). Finally, we note, that selenate analogue of alunogen, $Al_2(SeO_4)_3(H_2O)_{16}$, was reported in monoclinic space group $P2_1$ (Table 1) [Krivovichev, 2006].

Table 1. Literature data on crystallographic parameters of alunogen and related phases obtained from alunogen upon cooling and heating.

	Alunogen	Alunogen	Synthetic analogue	Selenate analogue	Low-temperature modification	Dehydrated modification
Chemical formula, $[Al(H_2O)_6]_2(TO_4)_3\times nH_2O$						
n, T	n = 4.4, T = S	n = 5, T = S	n = 4, T = S	n = 4, T = Se	n = 4.8, T = S	n = 1.8, T = S
Symmetry	Triclinic	Triclinic	Triclinic	Monoclinic	Monoclinic	Triclinic
Space group	P-1	P-1	P-1	$P2_1$	$P2_1$	P-1
a, Å	7.425	7.420	6.054	6.152	7.412	14.35
b, Å	26.975	26.970	7.424	27.445	26.834	12.49
c, Å	6.061	6.062	26.915	7.5650	6.078	6.09
α, °	90.03	89.57	88.047	90	90	92.66
β, °	97.66	97.34	89.948	97.93	97.31	96.65
γ, °	91.94	91.53	82.502	90	90	100.83
V, Å^3	1202.38	1202.73	1198.64	1265.09	1199.01	1062.8
Z	2	2	2	2	2	2
Genesis, locality	Natural from Vulcano, Italy	Natural from Königsber, Hungary	Synthetic	Synthetic	Colling of synthetic sample	Heating of synthetic sample
Reference	Menchetti, Sabelli, 1974	Fang, Robinson, 1976	Sun et al., 2015	Krivovichev, 2006	Khalenberg et al., 2015	Khalenberg et al., 2017

Thus, we can conclude that all previous structural studies carried out for natural and synthetic alunogen have shown the variability of the alunogen framework in relation to the number of "zeolite" H_2O molecules, as well as the possibility of changing the symmetry and unit-cell parameters of the mineral depending on the composition, mainly determined by the H_2O content, which presumably may even correspond not to alunogen, but to its meta-forms. At the same time, alunogen is a common mineral in geothermal fields, which often act as a proxy for Martian conditions. In particular, alunogen is widely distributed in the geothermal fields of Kamchatka [Zhitova et al., 2018, 2022, 2023a,b], which is one of the most active volcanic areas in the world and belongs to the zone of the Pacific Ring of Fire. At the same time, the crystal structure of alunogen from geothermal fields worldwide or from Kamchatka has not been previously studied. Our work is intended to fill this gap and analyse the crystal structure of natural alunogen from the standpoint of modern X-ray diffraction analysis.

Preprints (www.preprints.org) | NOT PEER-REVIEWED | Posted: 10 May 2023 doi:10.20944/preprints202305.0681.v1

2. Materials and Methods

2.1. Materials

In this study, we investigated the sample of alunogen collected from the surface of Verkne-Koshelevsky geothermal field associated with Koshelev volcano (South Kamchatka) (Figure 2a). South Kamchatka is a part of the Kuril-Kamchatka Island arc system, it is characterized by high tectonic-magmatic activity, which is expressed on the surface by modern volcanism. The Verkhne-Koshelevsky geothermal field is located in the central part of the Koshelev volcanic complex (Figure 2b) in an erosion crater at absolute heights of 1200–1250 meters. On the area of the field, especially in its northern part, large-block deluvial deposits are developed and, almost throughout the entire area of the field, argillic rocks are widely developed, which are the product of hydrothermal transformation of basaltic andesites. Thermal manifestations are represented by steam-gas jets (Figure 2c), water-mud boilers, hot springs and lakes, steaming ground. Thermal waters are characterized by temperature up to 95 °C, pH = 1.9–4.9, Eh = +60…+325 mV [Vakin et al., 1976; Kalacheva et al., 2016].

The sample was collected from the surface of 40 × 40 cm. The temperature of the ground in the sampling point was slightly elevated (retrospectively rated as ~ 40 °C) since the measured temperature at the depths of 30 cm was 80 °C. The sample was represented by white polymineral efflorescent crust up to 1.5 cm thick (Figure 2d) composed of different hydrated sulfate minerals. In the crust colourless tabular crystals of alunogen were separated using binocular microscope and subjected to structure study. The associated minerals include Fe-Al and Fe sulfates: halotrichite, metavoltine and voltaite-group mineral. The efflorescent was covering pyrite-rich zone of the argillizites (Figure 2d). The description of halotrichite from this locality is provided recently [Zhitova et al., 2023a,b].

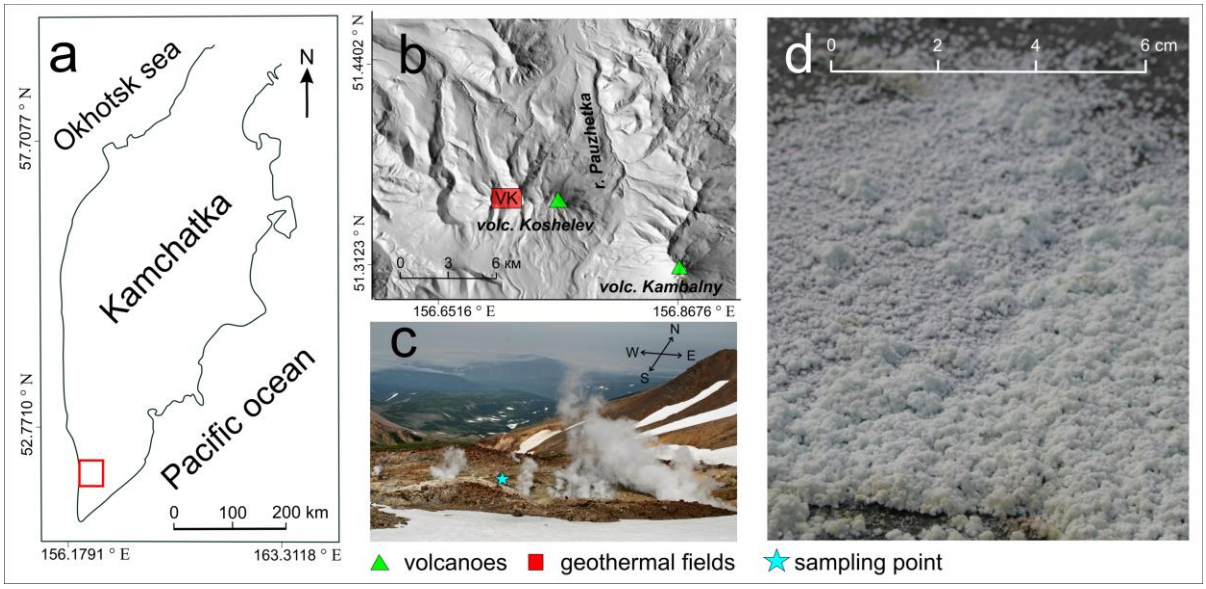

Figure 2. The place of sample collection: (**a**) position of Verkhne-Koshelevsky geothermal field at the map of Kamchatka; (**b**) the position of Verkhne-Koshelevsky geothermal field relative to Kochelev and Kambalny volcanoes (both active); (**c**) the general view to Verkhne-Koshelevsky geothermal field, steaming jets are visible; (**d**) the efflorescent polymineral crust composed of hydrated sulfates on the Verkhne-Koshelevsky geothermal field surface.

2.1. Methods

2.1.1. Scanning electron microscopy and Energy-dispersive X-ray spectroscopy

The chemical composition of alunogen was analyzed at the "Geomodel'" Resource Center of the Scientific Park of St. Petersburg State University on a Hitachi S-3400N scanning electron microscope,

 doi:10.20944/preprints202305.0681.v1

equipped with an Oxford X-Max 20 energy-dispersive spectrometer, at an accelerating voltage of 20 kV, a probe current of 0.5 nA with various electron beam diameters of minimum 5 μm due to fast dehydration of alunogen under the electron beam. The spectrometer was calibrated against the set of natural standards (MAC standards). The alunogen plates were deposited on carbon tape, carbon-coated and analyzed by SEM and EDS. The previous studies of hydrated metal sulfates and fumarolic minerals has indicated an advantage of using the energy-dispersive mode instead of the wave-dispersive mode for their analysis [Balic-Žunic et al., 2016; Kruszewski, 2013; Zhitova et al., 2022] due to lower probe current and shorter time of analysis that both contribute to the preservation of material under study. In addition, energy-dispersive spectroscopy (EDS) allows analysing small-size grains of distinct minerals found in intimate association and *in situ* control of the sample condition during the spectrum acquisition.

2.1.2. Single-crystal X-ray diffraction

Single-crystal X-ray diffraction analysis was carried out for alunogen using a four-circle diffractometer Rigaku XtaLAB Synergy-S (Oxford Diffraction, Japan) operated with a monochromated Mo$K\alpha$ radiation (source: Mo$K\alpha$, λ = 0.71073 Å) at 50 kV and 1.0 mA and equipped with a CCD HyPix-6000HE detector. The scan width was 1.0°, exposition was 130 s. Long exposure time is due to extremely small crystal thickness and relatively weak diffraction. The CrysAlisPro [CrysAlisPro, 2015] software package was used to process the data; an empirical absorption correction was calculated based on spherical harmonics implemented in the SCALES ABSPACK algorithm. Numerous attempts were undertaken in order to collect the single-crystal X-ray diffraction data of reasonable quality for structure refinement and hydrogen localization. These are because alunogen crystals are thin, maybe intergrown, twinned or low-crystalline. A photograph of the crystal on a nylon loop was taken during the analysis and given in the Supplementary File (Figure S1a), as well as one of the frames of collected single-crystal X-Ray diffraction data (Figure S1b). The parameters of data collection are listed in Table 2.

The structure was solved and refined using the ShelX program package [Sheldrick, 2015] incorporated into the Olex2 software shell [Dolomanov et al., 2009] to R_1 = 0.068 based on 5112 unique observed reflections with $I > 2\sigma(I)$.

Table 2. Crystal data, data collection, and structure refinement details for alunogen.

Crystal system	Triclinic
Space group	*P*-1
a (Å)	7.4194(3)
b (Å)	26.9763(9)
c (Å)	6.0549(2)
α (°)	90.043(3)
β (°)	97.703(3)
γ (°)	91.673(3)
V (Å^3)	1200.41(7)
Z	2
Calculated density (g/cm^3)	1.732
Absorption coefficient	0.496
Diffractometer	Rigaku XtaLAB Synergy-S
Temperature (K)	293
Radiation, wavelength (Å)	Mo$K\alpha$, 0.71073
Range of data collection, 2θ (°)	6.392 – 59.998
h, *k*, *l* ranges	-10→10, -37→37, -8→8
Total reflection collected	21599
Unique reflections (R_{int})	6985 (0.0408)
Number of unique reflections $F > 2\sigma(F)$	5112
Data completeness (%)	99.1

Preprints (www.preprints.org) | NOT PEER-REVIEWED | Posted: 10 May 2023 doi:10.20944/preprints202305.0681.v1

Refinement method	Full-matrix least-squares on F^2
Weighting coefficients a, b	0.0842, 4.2534
Data/ restrain/ parameters	6985/23/356
R_1 [$F > 2\sigma(F)$], wR_2 [$F > 2\sigma(F)$]	0.0680, 0.1830
R_1 all, wR_2 all	0.0947, 0.1981
Goodness-of-fit on F^2	1.049
Largest diff. peak and hole (ēÅ^{-3})	1.41/-0.62

2.1.3. Structure complexity

The structural complexity of alunogen and related phases were estimated using the approach of numerical evaluation of structural complexity developed by Krivovichev [Krivovichev 2012, 2013]. The complexity of crystal structure can be quantitatively characterized by the amount of Shannon information measured in bits (binary digits) per atom (I_G, bits/atom) and per unit cell ($I_{G,total}$, bits/cell), respectively, according to the following equations:

$$I_G = -\sum_{i=1}^{k} p_i \log_2 p_i \quad \text{(bits/atom)},$$

$$I_{G,total} = -v\, I_G = -v\sum_{i=1}^{k} p_i \log_2 p_i \quad \text{(bits/cell)},$$

where k is the number of different crystallographic orbits (independent crystallographic Wyckoff sites) in the structure and p_i is the random choice probability for an atom from the i-th crystallographic orbit, that is:

$$p_i = m_i / v,$$

where m_i is a multiplicity of a crystallographic orbit (i.e. the number of atoms of a specific Wyckoff site in the reduced unit cell), and v is the total number of atoms in the reduced unit cell. It worth to note, that the I_G value provides a negative contribution to the configurational entropy (S^{cfg}) of crystalline solids in accordance with the general principle that the increase in structural complexity corresponds to the decrease of configurational entropy [Krivovichev, 2016]. Structural complexity was calculated using previously published crystal structure models (*cif*-files) listed in Table 1 and program package ToposPro [Blatov et al., 2014].

3. Results

3.1. Chemical composition

The chemical composition of alunogen is given in Table 3. The EDS spectra of alunogen shows presence of Al, S and O in its compositions. The contents of other elements with atomic numbers higher than that of C are below their detection limits. Alunogen dehydrates under vacuum conditions which is manifested by the cracking of crystals and a decrease in water content that is, an increase in the measured amount of Al_2O_3 and SO_3 oxides. The contents of Al_2O_3 and SO_3 oxides were measured. The H_2O content has been calculated taking into account the crystal structure data (see below). The analyses were normalized to 100 wt. %. The analyses (Table 3) show a good agreement with alunogen stoichiometry since Al:S ~ 2:3

Table 3. Chemical composition of alunogen.

Constituent	Wt.%	apfu [1]
Al_2O_3	16.64	2.04
SO_3	37.88	2.96
H_2O	45.48	15.8
Total	100.00	-

[1] Atom per formula unit. Note: the chemical formula of the sample under study is $Al_2(SO_4)_3 \times 15.8\ H_2O$.

3.2. Crystal structure

The obtained data were processed in *P*-1 space group, a = 7.4194(3), b = 26.9763(9), c = 6.0549(2) Å, α = 90.043(3), β = 97.703(3), γ = 91.673(3) °, V = 1200.41(7) Å^3, Z = 2. Atom coordinates, site

Preprints (www.preprints.org) | NOT PEER-REVIEWED | Posted: 10 May 2023 doi:10.20944/preprints202305.0681.v1

occupancies and isotropic displacement parameters are given in Table 4. Selected bond lengths are listed in Table 5. Hydrogen bonding scheme is given in Table 6. Anisotropic displacement parameters are in Supplementary File (Table S1). The crystallographic information file (cif) has been deposited via the joint Cambridge Crystal Data Centre CCDC/FIZ Karlsruhe deposition service.

Table 4. Atom coordinates, equivalent isotropic displacement parameters (Å²) and site occupancies for alunogen.

Atom	*x*	*y*	*z*	U_{eq}	s.o.f.*
Al1	0.78185(17)	0.09886(4)	0.50210(19)	0.0167(2)	1
Al2	0.7633.8(17)	0.40035(4)	0.49664(19)	0.0152(2)	1
S1	0.26873(14)	0.06032(4)	0.01951(16)	0.0195(2)	1
S2	0.8767(2)	0.25246(5)	0.0304(2)	0.0373(3)	1
S3	0.25792(14)	0.43956(4)	0.01326(16)	0.018.(2)	1
O1	0.7331(4)	0.07010(11)	0.2166(5)	0.0208(6)	1
H1A	0.629562	0.077332	0.129221	0.070(20)	1
H1B	0.726442	0.037102	0.203752	0.043(17)	1
O2	0.5469(4)	0.07816(12)	0.5602(5)	0.0253(6)	1
H2A	0.514433	0.077916	0.689613	0.038	1
H2B	0.484467	0.054801	0.490644	0.038	1
O3	0.8734(4)	0.03768(10)	0.6112(5)	0.0212(6)	1
H3A	0.987721	0.035292	0.677682	0.028(14)	1
H3B	0.798441	0.015192	0.663402	0.060(20)	1
O4	0.8327(5)	0.12538(11)	0.7909(5)	0.0242(6)	1
H4A	0.922831	0.112312	0.882852	0.060(20)	1
H4B	0.816461	0.155182	0.849011	0.036(16)	1
O5	0.6910(5)	0.15850(12)	0.3869(6)	0.0292(7)	1
H5A	0.755229	0.169346	0.289779	0.044	1
H5B	0.705253	0.180607	0.489091	0.044	1
O6	0.6723(5)	0.33977(12)	0.3726(5)	0.0269(7)	1
H6A	0.557522	0.333332	0.315609	0.060(20)	1
H6B	0.745632	0.320012	0.31037	0.080(30)	1
O7	0.5278(4)	0.41786(12)	0.5461(5)	0.0237(6)	1
H7A	0.477642	0.417182	0.672458	0.060(20)	1
H7B	0.445572	0.434082	0.450818	0.080(30)	1
O8	0.7227(4)	0.43029(11)	0.2133(5)	0.0212(6)	1
H8A	0.617753	0.423902	0.122989	0.024(13)	1
H8B	0.734013	0.462642	0.192039	0.032(15)	1
O9	0.8591(4)	0.46183(11)	0.6180(5)	0.0223(6)	1
H9A	0.975952	0.464422	0.681249	0.030(15)	1
H9B	0.782732	0.482812	0.667619	0.024(13)	1
O10	0.0003(4)	0.38597(12)	0.4492(5)	0.0241(6)	1
H10A	0.046469	0.359188	0.50095	0.036	1
H10B	0.028361	0.38766	0.317745	0.036	1
O11	0.0199(4)	0.11697(12)	0.4490(5)	0.0251(6)	1
H11A	0.068681	0.107622	0.328402	0.050(20)	1
H11B	0.041821	0.147012	0.507622	0.100(30)	1
O12	0.8036(4)	0.37269(11)	0.7830(5)	0.0228(6)	1
H12A	0.900811	0.385322	0.86682	0.040(17)	1
H12B	0.784091	0.341862	0.82899	0.049(19)	1
O13	0.1265(5)	0.09455(14)	0.0551(6)	0.0330(8)	1
O14	0.1975(5)	0.02533(13)	0.1607(6)	0.0344(8)	1
O15	0.3266(5)	0.03353(14)	0.2275(6)	0.0353(8)	1

 doi:10.20944/preprints202305.0681.v1

O16	0.4281(5)	0.08828(13)	0.0448(5)	0.0279(7)	1
O17	0.0547(8)	0.2527(2)	0.0519(9)	0.0734(15)	1
O18	0.8967(7)	0.27314(17)	0.2560(8)	0.0571(13)	1
O19	0.7446(8)	0.28140(17)	0.1156(9)	0.0664(15)	1
O20	0.8074(8)	0.20139(14)	0.0374(7)	0.0581(14)	1
O21	0.4094(4)	0.41111(12)	0.0537(5)	0.0254(6)	1
O22	0.1939(5)	0.47437(12)	0.1653(6)	0.0323(8)	1
O23	0.1077(5)	0.40518(13)	0.0516(5)	0.0280(7)	1
O24	0.3261(5)	0.46681(13)	0.2206(5)	0.0310(7)	1
Ow25	0.3442(10)	0.3054(3)	0.2757(17)	0.112(4)	0.938(19)
H25A	0.405511	0.284882	0.359081	0.168	0.938(19)
H25B	0.324039	0.29113	0.149356	0.168	0.938(19)
Ow26	0.2092(8)	0.32520(18)	0.7034(9)	0.0600(13)	1
H26A	0.253358	0.334482	0.83401	0.090	1
H26B	0.231035	0.29443	0.700003	0.090	1
Ow27	0.5093(9)	0.2186(3)	0.5909(12)	0.073(3)	0.828(16)
H27A	0.584529	0.235869	0.680159	0.109	0.828(16)
H27B	0.486283	0.193019	0.665419	0.109	0.828(16)
Ow28**	0.1137(9)	0.2089(2)	0.5554(11)	0.0426(14)	0.65
H28A	0.071602	0.227891	0.450088	0.064	0.65
H28B	0.228548	0.213117	0.564612	0.064	0.65
Ow29**	0.2236(18)	0.1790(5)	0.7460(20)	0.050(3)	0.35
H29A	0.3004	0.187195	0.659704	0.075	0.35
H29B	0.273149	0.188686	0.874557	0.075	0.35

* All occupancies are fixed since their refined occupancy is close to 100%, except for O25 and O27 oxygen sites of H_2O molecules.

**O28 and O29 are disordered oxygen atoms of the one of "zeolite" H_2O molecules.

The two Al sites, three S sites and twenty-nine O sites were localized from the difference Fourier maps and refined anisotropically. Site occupancies of Al, S, O are given in Table 4 and they are all fully occupied with the exception of two oxygen positions (Ow25 and Ow27) of "zeolite" H_2O molecules. The two-component twinning by matrix {-1 0 0 0 1 0 0 0 -1} was applied to the structure refinement. The hydrogen positions were localized from the difference Fourier maps for nine H_2O molecules of $Al(H_2O)_6$ octahedra or taking into account geometrical assumptions for other three H_2O molecules of $Al(H_2O)_6$ octahedra and for all four "zeolite" H_2O molecules. In the first case the O–H distances were softly restrained as 0.9 Å. Some of O···H and H···H distances were also softly restrained as 2.4-2.5 Å. All thirty-four H sites were located (Figure 3a) and refined isotropically with and Ueq refined freely for H atoms of nine out of twelve H_2O molecules of $Al(H_2O)_6$ octahedra and using a riding model with Ueq values restrained as 1.5 of donor O atom for H atoms of the other three H_2O molecules of $Al(H_2O)_6$ octahedra and for all "zeolite" H_2O molecules. Additionally, one "zeolite" H_2O molecule is disordered and split into two partially occupied sites: Ow28 and Ow29 (Figure 3b) located at the distance of 1.56 Å with occupancies 0.65 and 0.35 correspondingly.

Preprints (www.preprints.org) | NOT PEER-REVIEWED | Posted: 10 May 2023 doi:10.20944/preprints202305.0681.v1

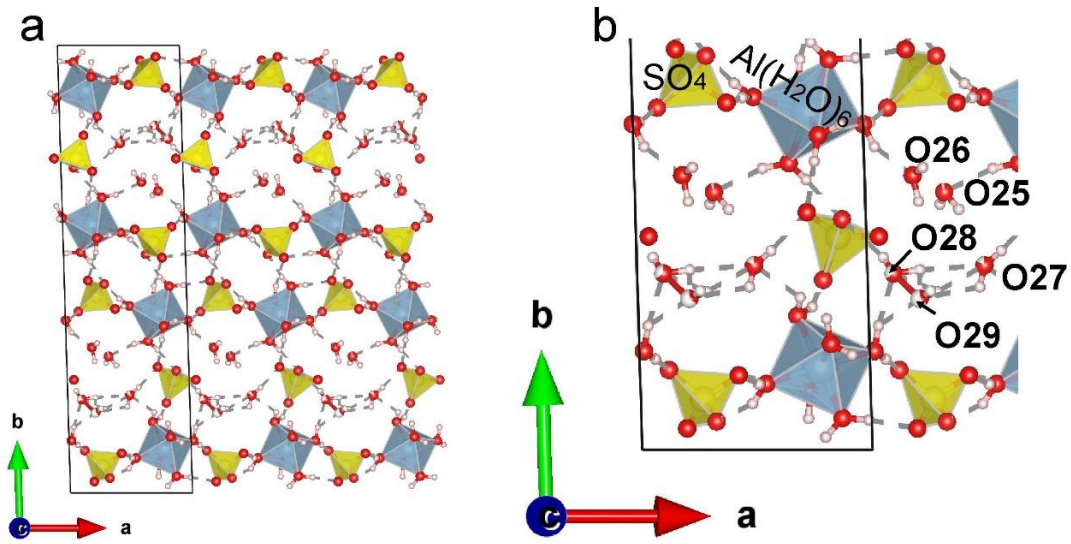

Figure 3. The crustal structure of alunogen obtained therein: (**a**) the framework showing H sites and hydrogen bonding scheme; (**b**) enlarged part showing labelling of "zeolite" H_2O molecules and disordering of one of them producing two partially occupied sites: O28 and O29.

Table 5. Selected bond lengths for alunogen.

Bond	Distance (Å)	Bond	Distance (Å)
Al–O1	1.880(3)	S1–O13	1.460(3)
Al1–O2	1.893(3)	S1–O14	1.475(3)
Al1–O3	1.889(3)	S1–O15	1.472(3)
Al1–O4	1.875(3)	S1–O16	1.480(3)
Al1–O5	1.862(3)	**<S–O>**	**1.472**
Al1–O11	1.888(3)		
<Al1-O>	**1.881**	S2–O17	1.473(5)
		S2–O18	1.462(4)
Al2–O6	1.868(3)	S2–O19	1.471(5)
Al2–O7	1.886(3)	S2–O20	1.459(4)
Al2–O8	1.888(3)	**<S2–O>**	**1.467**
Al2–O9	1.893(3)		
Al2–O10	1.871(3)	S3–O21	1.479(3)
Al2–O12	1.878(3)	S3–O22	1.472(3)
<Al2-O>	**1.881**	S3–O23	1.471(3)
		S3–O24	1.476(3)
		<S3–O>	**1.475**

The hydrogen bonding scheme in alunogen is complex. The oxygen atoms labeled O1, O2…O12 are coordinating Al1 and Al2 octahedra being donors (**D**) of two-center hydrogen bonds [Jeffrey, 1997]. The **D**–H bonds are in the range 0.85-0.90 Å (Table 6). The oxygen atoms of the sulfate tetrahedra and "zeolite" H_2O molecules act as an acceptor. For the case when the oxygen of the sulfate group is the acceptor (**A**), the following H···**A** distances are characteristic 1.70–1.92 Å and **D**–H···**A** angles in the range 147.8–179.5 º (with averaged values as 1.79 Å and 167.9 º, respectively). When oxygen of "zeolite" H_2O molecules is an acceptor, the H···**A** distances range from 1.72 to 2.02 Å and **D**–H···**A** angles are in the range 125.4–163.9 º (with averaged values as 1.86 Å and 147.5 º, respectively).

The oxygen atoms labeled Ow25, Ow26, Ow27 and Ow28 + Ow29 (split) belong to "zeolite" H_2O molecules. For this type of H_2O molecules, the **D**–H bonds are ~ 0.85 Å. The oxygen atoms of SO_4 tetrahedra and symmetrically independent "zeolite" H_2O molecules act as acceptors. In case when O

Preprints (www.preprints.org) | NOT PEER-REVIEWED | Posted: 10 May 2023 doi:10.20944/preprints202305.0681.v1

atoms of SO_4 are acceptors the H···**A** distances range from 1.99 to 2.72 Å (with the average value of 2.37 Å) and **D**–H···**A** angles are in the range 108.1–174.7 º (with averaged value of 136.1 °). When oxygen of "zeolite" H_2O molecules is an acceptor, the H···**A** distances range from 1.84 to 2.55 Å (average value is 2.18 Å) and **D**–H···**A** angles ranging from 120.4 to 176.4 ° (average value is 152.7 °).

Table 6. Hydrogen bonding scheme for alunogen.

D–H	*d*(**D**–H), Å	*d*(H···**A**), Å	<**DHA**, °	*d*(**D**···A) , Å	**A**
O1-H1A	0.90	2.65	116.7	3.155(5)	O15
		1.74	177.1	2.640(4)	O16
O1-H1B	0.89	1.82	158.0	2.670(4)	O14
O2-H2A	0.85	1.83	169.7	2.674(4)	O16
O2-H2B	0.85	1.92	147.8	2.679(5)	O15
O3-H3A	0.89	2.85	121.7	3.402(4)	O13
		1.75	171.2	2.638(4)	O14
		2.93	100.8	3.221(6)	O3
O3-H3B	0.90	1.77	173.3	2.659(4)	O15
O4-H4A	0.89	1.79	170.5	2.678(5)	O13
		2.83	101.8	3.141(4)	O1
O4-H4B	0.90	1.70	161.1	2.561(5)	O20
O5–H5A	0.85	1.84	157.9	2.646(5)	O20
O5-H5B	0.85	1.97	125.4	2.557(7)	Ow27
		3.08	105.8	3.409(7)	Ow28
O6-H6A	0.89	1.72	160.1	2.572(8)	Ow25
O6-H6B	0.89	1.77	164.9	2.644(5)	O18
		2.78	134.2	3.460(7)	O19
O7-H7A	0.89	1.80	170.8	2.691(4)	O21
O7-H7B	0.90	1.80	166.1	2.683(4)	O24
O8-H8A	0.90	1.78	179.5	2.685(4)	O21
		2.62	117.3	3.136(5)	O24
O8-H8B	0.89	1.78	168.0	2.653(4)	O22
O9-H9A	0.90(1)	1.767(11)	172.0(14)	2.661(4)	O22
		2.837(14)	121.2(11)	3.392(4)	O23
		3.033(15)	102.7(11)	3.348(6)	O9
O9-H9B	0.89	1.78	167.4	2.657(4)	O24
O10-H10A	0.85	2.87	112.8	3.293(6)	O18
		1.86	151.2	2.640(6)	Ow26
O10-H10B	0.85	1.85	167.4	2.681(4)	O23
O11-H11A	0.90	1.80	168.3	2.685(4)	O13
O11-H11B	0.89	1.75	163.9	2.613(7)	Ow28
		2.02	136.7	2.729(12)	Ow29
O12-H12A	0.88	1.84	174.2	2.721(4)	O23
		3.11	101.5	3.397(6)	Ow26
O12-H12B	0.89	1.69	173.3	2.578(5)	O19
Ow25-H25A	0.85	2.36	166.7	3.190(13)	Ow27
Ow25-H25B	0.85	2.40	132.3	3.042(10)	O17
Ow26-H26A	0.85	2.39	128.1	2.991(6)	O21
		2.65	122.5	3.191(6)	O23
Ow26-H26B	0.85	2.38	108.1	2.769(7)	O17
		2.55	145.8	3.292(8)	Ow28
Ow27-H27A	0.85	1.99	174.7	2.841(8)	O19

Preprints (www.preprints.org) | NOT PEER-REVIEWED | Posted: 10 May 2023 doi:10.20944/preprints202305.0681.v1

		2.72	126.2	3.298(9)	O20
Ow27-H27B	0.85	2.10	120.4	2.631(14)	Ow29
Ow28-H28A	0.85	2.06	160.6	2.875(8)	O18
Ow28-H28B	0.85	2.07	176.4	2.918(9)	Ow27
Ow29-H29A	0.85	1.84	154.0	2.631(14)	Ow27
Ow29-H29B	0.85	2.48	99.3	2.752(15)	O17

An analysis of the distribution of hydrogen bonds shows that a stronger H···**A** bonds observed for H_2O molecules coordinating Al sites. At the same time, the sulfate group is a stronger acceptor resulting in a stronger hydrogen bond between the $Al(H_2O)_6$ octahedra and the SO_4 tetrahedra. "Zeolite" H_2O molecules are characterized by longer (and hence weaker) bonds with acceptors. Moreover, in case of "zeolite" H_2O molecule a stronger hydrogen bond is formed with other symmetrically independent "zeolite" H_2O molecules rather than SO_4 tetrahedra. The formation of stronger hydrogen bonds between "zeolite" H_2O molecules rather than its bonding with other structural units, in our opinion, explains the possibility of alunogen dehydration and possible formation of meta-alunogen.

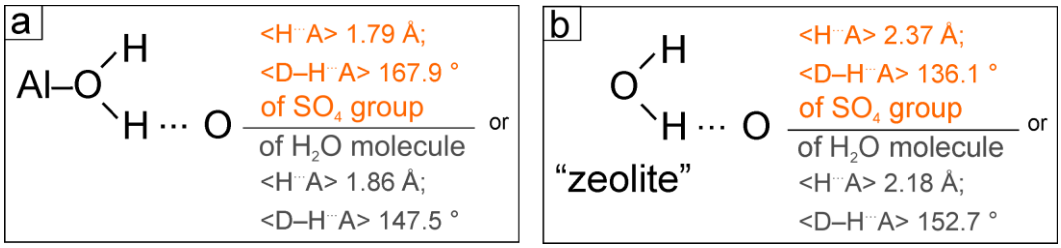

Figure 4. The averaged parameters of hydrogen bonding represented by H···**A** bonds and **D**–H···**A** angles of (**a**) $Al(H_2O)_6$ octahedra linked to SO_4 tetrahedra or "zeolite" H_2O molecule and (**b**) "zeolite" H_2O molecules linked to SO_4 tetrahedra or symmetrically independent "zeolite" H_2O molecule.

3.1. Structure complexity

Crystal structure complexity of alunogen and related phases is shown in Table 7. The parameters I_G and $I_{G,total}$ correspond to the complexity calculated for the structural models per atom and per unit cell. Examination of the values in the Table 7 shows their division into two groups: (i) I_G ~ 5.0–5.1 bits/atom and $I_{G,total}$ ~ 333–346 bits/cell and (ii) I_G ~ 6.0–6.1 bits/atom and $I_{G,total}$ ~ 783–828 bits/cell. Such a difference is due to the fact that earlier structure refinements do not contain H positions. Thus, hydrogen atoms contribute to more than a half of structure complexity of alunogen that is in line with high hydration state of alunogen having ~ 45 wt. % of H_2O (Table 2). Table 7 also shows obvious correlation between number of O sites corresponding to "zeolite" H_2O molecules. For example, considering the crystal structures with non-localized H atoms, the complexity per unit cell is 333 bits/cell for selenate alunogen with four O sites corresponding to "zeolite" H_2O molecules and 346 bits/cell for natural alunogens having five fully or partly occupied O sites corresponding to "zeolite" H_2O molecules. The same applies to the structures with localized H sites: the synthetic alunogen with n (number of "zeolite" H_2O molecules) = 4 has complexity per unit cell as 783 bits/cell, while low-temperature monoclinic modification with n = 4.8 has 828 bits/cell. In our structure refinement n = 3.8, but one of "zeolite" H_2O molecules is split into two with partial occupancy that leads to the identical complexities of our sample and low-temperature modification. This is also interesting to note that transformation from triclinic to monoclinic symmetry is not outlined by a change of structure complexity. This is because the structure topology is preserved. We were unable to find a cif-file for dehydrated modification of alunogen. However, we can assume that it should have lower complexity since it has lower content of "zeolite" H_2O molecules.

Preprints (www.preprints.org) | NOT PEER-REVIEWED | Posted: 10 May 2023 doi:10.20944/preprints202305.0681.v1

Table 7. Crystal structure parameters and information complexities (I_G; $I_{G,total}$) of alunogen and related phases.

	Alunogen	Alunogen	Alunogen	Synthetic analogue	Selenate analogue	Low-temperature modification
Chemical formula, $[Al(H_2O)_6]_2(TO_4)_3 \times nH_2O$						
n, T	n = 3.8 [1], T = S	n = 4.4, T = S	n = 5, T = S	n = 4, T = S	n = 4, , T = Se	n = 4.8, , T = S
H-positions in cif-file	Located	Non-located	Non-located	Located	Non-located	Located
Symmetry	Triclinic	Triclinic	Triclinic	Triclinic	Monoclinic	Monoclinic
Space group	P-1	P-1	P-1	P-1	$P2_1$	$P2_1$
I_G, bits/atom	6.1	5.1	5.1	6.0	5.0	6.1
$I_{G,total}$ bits/cell	828	346	346	783	333	828
Reference	This research	Menchetti, Sabelli, 1974	Fang, Robinson, 1976	Sun et al., 2015	Krivovichev, 2006	Khalenberg et al., 2015

[1] one position of "zeolite" H_2O molecule is disordered and split to O28 and O29.

4. Discussion

In our study alunogen comes from Fe-rich (both ferric and ferrous) environment and found in intimate association with other Fe or Fe-Al hydrated sulfates. At the same time, Fe^{3+} does not incorporate in the structure of alunogen studied therein. Following ideas of Fang and Robinson [Fang, Robinson, 1976] we conclude that the difference in the ionic size and polarization power should be responsible for that rather than non-availability of Fe^{3+}. We can assume that even if some (limited) Al to Fe^{3+} substitution occurs in individual alunogen crystals, it should have a negative effect on the crystallinity of the alunogen precluding its structural study. It is interesting to note, that according to our data, limited Al to Fe^{3+} substitution occurred in other hydrated sulfates from geothermal fields: alums and alunite/jarosite-group minerals where formation of Fe^{3+}- or Al-dominant species in intimate association was observed rather than their full solid solution series [Zhitova et al., 2022] and halotrichite where Al site was free of impurities or contained limited Fe^{3+} [Zhitova et al., 2023a,b]. If terrestrial geothermal fields are indeed a proxy for Martian conditions [Pirajno, Van Kranendonk, 2005], then there should be not only iron sulfates, already well known for Mars, but also aluminum sulfates, and it can be assumed that alunogen or its modifications maybe widespread (following mineral formation at geothermal fields). The alunogen described by us contains the smallest amount of "zeolite" H_2O molecules (3.8 *apfu vs* 4–5 *apfu*) among structurally characterized natural and synthetic minerals. Despite the structural study of alunogen, including low- and high-temperature modifications [Kahlenberg et al., 20015, 2017], the question seems to be open on whether alunogen with different content of "zeolite" H_2O molecules will behave identically under low-temperature conditions that are modelling Martian environments?

In this work we provide modern crystal structure refinement of alunogen including the first localization of thirty-four hydrogen sites. Each of Al and S sites has shown 100 % occupancy. The structure consists of isolated $Al(H_2O)_6$ octahedra, SO_4 tetrahedra and "zeolite" H_2O molecules that are connected to the three-dimensional network by hydrogen bonds. The hydrogen atoms form two-centre hydrogen bonds of $Al(H_2O)_6$ octahedra and "zeolite" H_2O molecules. Four sites corresponding to "zeolite" H_2O molecules were localized (including O and H atoms) with one "zeolite" H_2O molecule being disordered and split. Analysis of hydrogen bonding network explains possibility of

 doi:10.20944/preprints202305.0681.v1

alunogen dehydration since independent "zeolite" H_2O molecules form stronger hydrogen bonding to each other rather than to other acceptors. The detailed information on hydrogen bonding network should be helpful for band assignments in the vibration spectra of alunogen and its modifications that is in demand in connection with studies of Martian mineralogy by rovers and the development of remote and express methods of terrestrial minerals identification [Košek et al., 2018]. In general, crystal structure of alunogen shows variability only in the content of "zeolite" H_2O molecules outlined by the consistency of the unit-cell volume (Tables 1 and 2) that possibly can be regarded as structure inflexibility towards isomorphic substitution.

Hydrogen sites contribute significantly to the structure complexity of alunogen increasing structure complexity per unit cell from 346 to 828 bits/cell. An increase in structure complexity by a factor of two or more due to hydrogen positions is also characteristic of other hydrated sulfates occurring in association with alunogen [Zhitova et al., 2023a]. This is because the crystal structure of alunogen and other hydrated sulfates from the same association (e.g. halotrichite, alum-group minerals [Zhitova et al., 2019, 2022]) is built of isolated units (octahedra, tetrahedra and H_2O molecules) connected by hydrogen bonds. As suggested previously highly hydrated minerals are good candidates for better understanding of ionic species existing in solution [Fang, Robinson, 1976]. In general, low polymerization of structural units is characteristic for the main efflorescent minerals growing from hydrothermal solution, including alunogen. Taking into account the abundance of alunogen at geothermal fields and recent experiments of transformation of alunogen to meta-alunogen at 40-80 °C [Kahlenberg et al., 2015] we consider that possibility of meta-alunogen occurrence at geothermal and/or fumarole fields is high despite questionable mineral status of meta-alunogen.

5. Conclusions

We consider the crystal structure study of alunogen from Verkhne-Koshelevsky geothermal field is an important outcome for characterization of naturally occurring highly hydrated sulfate minerals and their possible modifications. The chemical specificity of alunogen from geothermal field are absence of impurities (including Fe^{3+} despite $Fe^{2+,3+}$-rich environment) and lower H_2O content in comparison to previously structurally characterized natural and synthetic alunogens. From the structural point of view alunogen studied in this work is isotypic to previously reported structures of alunogen. However, in addition to previous studies we were able to localize hydrogen atoms and characterize complex hydrogen bonding network of the mineral. This data maybe helpful for detailed assignment of band positions in the vibrational spectra and useful for Mars mineralogical missions. Hydrogen atoms increase structure complexity per unit cell more than twice similarly to other highly hydrated sulfates found in association with alunogen. Combining the recently obtained experimental data on the transition of alunogen to meta-alunogen at temperature ~ 40–80 °C and our field temperature measurements at geothermal and fumarole fields, we assume that the findings of meta-alunogen under low-temperature volcano-related conditions are very likely. At the same time, the structural study of alunogen from geothermal fields can be a starting point in the search and characterization of meta-alunogen or its possible structural varieties in nature.

Supplementary Materials: The following supporting information can be downloaded at the website of this paper posted on Preprints.org.

Author Contributions: Conceptualization, ESZ and RMS; methodology, RMS; software, ESZ, RMS, AAZ, AAN; validation, ESZ, RMS, AAZ, AAN; formal analysis, ESZ, RMS, AAZ; investigation, ESZ, RMS, AAN; resources, AAN; data curation, RMS, AAZ; writing—original draft preparation, ESZ, RMS, AAZ, AAN; writing—review and editing, ESZ, RMS, AAZ, AAN; visualization, ESZ; supervision, ESZ, AAZ; project administration, ESZ; funding acquisition, ESZ. All authors have read and agreed to the published version of the manuscript.

Funding: This research was funded by the Russian Science Foundation, grant number 22-77-10036.

Data Availability Statement: The crystallographic information file (cif) has been deposited via the joint Cambridge Crystal Data Centre CCDC/FIZ Karlsruhe deposition service.

Acknowledgments: The technical support of St. Petersburg State University Resource Centers "XRD" and "Geomodel" is gratefully acknowledged.

Conflicts of Interest: The authors declare no conflict of interest.

References

1. Beudant, F. S. Alunogène, sulfate d'alumine. *Traité Élémentaire de Minéralogie* **1832**, 2nd Edition, 488-492
2. Košek, F., Culka, A., Žáček, V., Laufek, F., Škoda, R., Jehlička, J. Native alunogen: A Raman spectroscopic study of a well-described specimen. *J. Mol. Struct.* **2018,** *1157*, 191-200.
3. Bariand, P., Cesbron, F., Berthelon, J-P. Les sulfates de fer de Saghand près de Yazd (Iran). *Mémoire Hors-Série de la Société Géologique de France*. **1977**, *8*, 77-85.
4. Biagioni, C., Mauro, D., Pasero, M. Sulfates from the pyrite ore deposits of the Apuan Alps (Tuscany, Italy). *A review. Minerals* **2020**, *10*, 1092.
5. Zhitova, E. S., Siidra, O. I., Belakovsky, D. I., Shilovskikh, V. V., Nuzhdaev, A. A., Ismagilova, R. M. Ammoniovoltaite, $(NH_4)_2Fe^{2+}_5Fe^{3+}_3Al(SO_4)_{12}(H_2O)_{18}$, a new mineral from the Severo-Kambalny geothermal field, Kamchatka, Russia. *Mineral. Mag.*, **2018**, *82(5),* 1057-1077.
6. Menchetti, S., Sabelli, C. Alunogen. Its structure and twinning. *Tschermaks Mineral. Petrogr. Mitt.* **1974**, *21,* 164-178.
7. Larsen, E. S., Steiger, G. Dehydration and optical studies of alunogen, nontronite and griffithite. *Am. J. Sci*. **1928**, *15*, 1-19.
8. Gordon, S. G. Results of the Chilean mineralogical expedition of 1938. Part VII. The crystallography of alunogen, meta-alunogen and pickeringite. *Notulae Naturae of The Academy of Natural Sciences of Philadelphia*, **1942,** *101,* 1-9.
9. Forti, P.; Panzica La Manna, M.; Rossi, A. The peculiar mineralogic site of the Alum cave (Vulcano, Sicily). In Proceedings of the 7th International Symposium on Vulcano speleology, Canary Islands, Spain, November 1994, p. 35-44.
10. Fang, J. H., Robinson, P. D. Alunogen, $Al_2(H_2O)_{12}(SO_4)_3{\cdot}5H_2O$: Its atomic arrangement and water content. *Am. Min*., **1976**, *61*, 311-317.
11. Sun, X., Sun, Y., Yu, J. Crystal structure of aluminum sulfate hexadecahydrate and its morphology. *Cryst. Res. Technol.*, **2015**, *50(4)*, 293-298.
12. Bibring, J.-P., Langevin, Y., Mustard, J.F., Poulet, F., Arvidson, R., Gendrin, A., Gondet, B., Mangold, N., Pinet, P., Forget, F. Global mineralogical and aqueous Mars history derived from OMEGA/Mars express data. *Sci*., **2006**, *312*, 400–404.
13. Swayze, G.A., Ehlmann, B.L., Milliken, R.E., Poulet, F., Wray, J.J., Rye, R.O., Clark, R.N., Desborough, G.A., Crowley, J.K., Gondet, B., Mustard, J. F., Seelos, K. D., Murchie, S. L. Discovery of the acid-sulfate mineral alunite in Terra Sirenum, Mars, using MRO CRISM: Possible evidence for acid-saline lacustrine deposits? *EoS Transactions of the American Geophysical Union,* Fall Meeting Supplement, **2008,** *89*, Abstract P44A-04.
14. Kounaves, S.P., Hecht, M.H., Kapit, J., Quinn, R.C., Catling, D.C., Clark, B.C., Ming, D.W., Gospodinova, K., Hredzak, P., McElhoney. K., Shusterman, J. Soluble sulphate in the martian soil at the Phoenix landing site. *Geophys. Res. Lett*., **2010**, *37(9)*, L09201.
15. Bish, D.L., Blake, D.F., Vaniman, D.T., Chipera, S.J., Morris, R.V., Ming, D.W., Treiman, A.H., Sarrazin, P., Morrison, S.M., Downs, R.T., and others and the MSL Science Team. X-ray diffraction results from Mars Science Laboratory: Mineralogy of Rocknest at Gale Crater. *Sci*., **2013**, *341*, 1238932.
16. Kahlenberg, V., Braun, D. E., Orlova, M. Investigations on alunogen under Mars-relevant temperature conditions: An example for a single-crystal-to-single-crystal phase transition. *Am. Min*., **2015**, *100(11-12)*, 2548-2558.
17. Kahlenberg, V., Braun, D. E., Krüger, H., Schmidmair, D., Orlova, M. Temperature-and moisture-dependent studies on alunogen and the crystal structure of meta-alunogen determined from laboratory powder diffraction data. *Phys. Chem. Miner*., **2017**, *44*, 95-107.
18. Krivovichev, S.V. Crystal chemistry of selenates with mineral-like structures. I. $(Al(H_2O)_6)_2(SeO_4)_3(H_2O)_4$—the selenate analog of alunogen. *Zapiski RMO,* **2006**, *135*, 106–113 (in Russian).
19. Zhitova, E. S., Siidra, O. I., Belakovsky, D. I., Shilovskikh, V. V., Nuzhdaev, A. A., Ismagilova, R. M. Ammoniovoltaite, $(NH_4)_2Fe^{2+}_5Fe^{3+}3Al(SO_4)_{12}(H2O)_{18}$, a new mineral from the Severo-Kambalny geothermal field, Kamchatka, Russia. *Mineral. Mag.*, **2018**, *82(5)*, 1057-1077.

20. Zhitova E.S., Sheveleva R.M., Zolotarev A.A., Krivovichev S.V., Shilovskikh V.V., Nuzhdaev A.A., Nazarova M.A. The crystal structure of magnesian halotrichite, (Fe,Mg)$Al_2(SO_4)_4 \cdot 22H_2O$: hydrogen bonding, geometrical parameters and structural complexity. *J. Geosci*. **2023**, *accepted*.
21. Sheveleva R.M., Nazarova M.A., Nuzhdaev A.A., Zhegunov P.S., Zhitova E.S. Distribution and chemical composition of halotrichite from the geothermal fields of Kamchatka. *Bulletin of Kamchatka Regional Association Educational-Scientific Center. Earth Sciences*. **2023**, *accepted (in Russian)*.
22. Vakin, E.A.; Dekusar, Z.B.; Serezhnikov, A.I.; Spichenkova, M.V. The hydrothermal occurrences of the Koshelevskii volcanic massif. Hydrothermal Systems and Thermal Fields in Kamchatka, Sugrobov, V.M., Eds.; Vladivostok: DVNTs AN SSSR, **1976**, pp. 58–84 (*in Russian*).
23. Kalacheva, E.G.; Rychagov, S.N.; Koroleva, G.P.; Nuzhdaev, A.A., The Geochemistry of Steam Hydrothermal Occurrences in the Koshelev Volcanic Massif, Southern Kamchatka. *J. Volcanol. Seismol*., **2016**, *3*, 41–56.
24. Balić-Žunić, T., Garavelli, A., Jakobsson, S. P., Jonasson, K., Katerinopoulos, A., Kyriakopoulos, K., Acquafredda, P. Fumarolic minerals: An overview of active European volcanoes. In *Updates in Volcanology, from Volcano Modelling to Volcano Geology*; Nemeth, K., Ed.; InTech: Rijeka, Croatia, 2016; pp. 267–322.
25. Kruszewski, Ł. Supergene sulphate minerals from the burning coal mining dumps in the Upper Silesian Coal Basin, South Poland. *Int. J. Coal Geol*., **2013**, *105*, 91-109.
26. *CrysAlisPro Software System*, version 1.171.38.46; Rigaku Oxford Diffraction: Oxford, UK, 2015.
27. Sheldrick, G.M. Crystal structure refinement with SHELXL. *Acta Crystallogr. A* **2015**, *71*, 3–8.
28. Dolomanov, O.V.; Bourhis, L.J.; Gildea, R.J.; Howard, J.A.; Puschmann, H. OLEX2: a complete structure solution, refinement and analysis program. *J. Appl. Crystallogr.* **2009**, *42(2)*, 339-341.
29. Krivovichev, S. Topological complexity of crystal structures: quantitative approach. *Acta Crystallogr. A*, **2012**, *68(3)*, 393-398.
30. Krivovichev, S. V. Structural complexity of minerals: information storage and processing in the mineral world. *Mineral.Mag*., **2013**, *77(3)*, 275-326.
31. Krivovichev, S. V. Structural complexity of minerals and mineral parageneses: Information and its evolution in the mineral world. In Highlights in mineralogical crystallography; Armbruster, T., Danisi. R.M. Eds.; Walter de Gruyter GmbH: Berlin, Germany, 2016; Volume 1, pp. 31-73.
32. Blatov, V. A., Shevchenko, A. P., Proserpio, D. M. Applied topological analysis of crystal structures with the program package ToposPro. *Crystal Growth & Design*, **2014**, *14(7)*, 3576-3586.
33. Jeffrey, G. A.; Jeffrey, G. A. *An introduction to hydrogen bonding*, Vol. 12; Oxford university press: New York, USA, 1997; pp. 1-228.
34. Pirajno, F.; Van Kranendonk, M. J. Review of hydrothermal processes and systems on Earth and implications for Martian analogues. *Australian Journal of Earth Sciences*, **2005**, *52(3)*, 329-351.
35. Zhitova, E.S.; Sergeeva, A.V.; Nuzhdaev, A.A.; Krzhizhanovskaya, M.G.; Chubarov, V.M. Tschermigite from thermal fields of Southern Kamchatka: High-temperature transformation and peculiarities of IR-spectrum. *Zapiski RMO*, **2019**, *148(1)*, 100-116.